BIOINORGANIC CHEMISTRY

A Short Course

Second Edition

ROSETTE M. ROAT-MALONE
Chemistry Department
Washington College
Chestertown, MD

WILEY-INTERSCIENCE
A John Wiley & Sons, Inc., Publication

BIOINORGANIC
CHEMISTRY

BICENTENNIAL
1807
WILEY
2007

The Wiley Bicentennial–Knowledge for Generations

Each generation has its unique needs and aspirations. When Charles Wiley first opened his small printing shop in lower Manhattan in 1807, it was a generation of boundless potential searching for an identity. And we were there, helping to define a new American literary tradition. Over half a century later, in the midst of the Second Industrial Revolution, it was a generation focused on building the future. Once again, we were there, supplying the critical scientific, technical, and engineering knowledge that helped frame the world. Throughout the 20th Century, and into the new millennium, nations began to reach out beyond their own borders and a new international community was born. Wiley was there, expanding its operations around the world to enable a global exchange of ideas, opinions, and know-how.

For 200 years, Wiley has been an integral part of each generation's journey, enabling the flow of information and understanding necessary to meet their needs and fulfill their aspirations. Today, bold new technologies are changing the way we live and learn. Wiley will be there, providing you the must-have knowledge you need to imagine new worlds, new possibilities, and new opportunities.

Generations come and go, but you can always count on Wiley to provide you the knowledge you need, when and where you need it!

William J. Pesce
William J. Pesce
President and Chief Executive Officer

Peter Booth Wiley
Peter Booth Wiley
Chairman of the Board

BIOINORGANIC CHEMISTRY

A Short Course

Second Edition

ROSETTE M. ROAT-MALONE
Chemistry Department
Washington College
Chestertown, MD

WILEY-INTERSCIENCE
A John Wiley & Sons, Inc., Publication

Copyright © 2007 by John Wiley & Sons, Inc. All rights reserved

Published by John Wiley & Sons, Inc., Hoboken, New Jersey
Published simultaneously in Canada

No part of this publication may be reproduced, stored in a retrieval system, or transmitted in any form or by any means, electronic, mechanical, photocopying, recording, scanning, or otherwise, except as permitted under Section 107 or 108 of the 1976 United States Copyright Act, without either the prior written permission of the Publisher, or authorization through payment of the appropriate per-copy fee to the Copyright Clearance Center, Inc., 222 Rosewood Drive, Danvers, MA 01923, (978) 750-8400, fax (978) 750-4470, or on the web at www.copyright.com. Requests to the Publisher for permission should be addressed to the Permissions Department, John Wiley & Sons, Inc., 111 River Street, Hoboken, NJ 07030, (201) 748-6011, fax (201) 748-6008, or online at http://www.wiley.com/go/permission.

Limit of Liability/Disclaimer of Warranty: While the publisher and author have used their best efforts in preparing this book, they make no representations or warranties with respect to the accuracy or completeness of the contents of this book and specifically disclaim any implied warranties of merchantability or fitness for a particular purpose. No warranty may be created or extended by sales representatives or written sales materials. The advice and strategies contained herein may not be suitable for your situation. You should consult with a professional where appropriate. Neither the publisher nor author shall be liable for any loss of profit or any other commercial damages, including but not limited to special, incidental, consequential, or other damages.

For general information on our other products and services or for technical support, please contact our Customer Care Department within the United States at (800) 762-2974, outside the United States at (317) 572-3993 or fax (317) 572-4002.

Wiley also publishes its books in a variety of electronic formats. Some content that appears in print may not be available in electronic formats. For more information about Wiley products, visit our web site at www.wiley.com.

Wiley Bicentennial logo: Richard J. Pacifico

Library of Congress Cataloging-in-Publication Data:

Bioinorganic chemistry : a short course / edited by Rosette M. Roat-Malone.—2nd ed.
p. ; cm.
Includes bibliographical references and index.
ISBN 978-0-471-76113-6 (pbk.)
1. Bioinorganic chemistry. I. Roat-Malone, Rosette M.
[DNLM: 1. Biochemistry. 2. Chemistry, Bioinorganic. QU 130 B614407 2008]
QP531.R63 2008
572′.51—dc22
2007019892

Printed in the United States of America

10 9 8 7 6 5 4 3 2 1

To my young friends
Allie, Andy, Anna, and Sebastian

CONTENTS

Preface xiii

Acknowledgments xix

1 Inorganic Chemistry Essentials 1

- 1.1 Introduction, 1
- 1.2 Essential Chemical Elements, 1
- 1.3 Metals in Biological Systems: A Survey, 3
- 1.4 Inorganic Chemistry Basics, 6
- 1.5 Biological Metal Ion Complexation, 8
  - 1.5.1 Thermodynamics, 8
  - 1.5.2 Kinetics, 9
- 1.6 Electronic and Geometric Structures of Metals in Biological Systems, 13
- 1.7 Bioorganometallic Chemistry, 19
- 1.8 Electron Transfer, 22
- 1.9 Conclusions, 26
- References, 27

2 Biochemistry Fundamentals 29

- 2.1 Introduction, 29
- 2.2 Proteins, 30
  - 2.2.1 Amino Acid Building Blocks, 30
  - 2.2.2 Protein Structure, 33

- 2.2.3 Protein Sequencing and Proteomics, 39
- 2.2.4 Protein Function, Enzymes, and Enzyme Kinetics, 43

2.3 Nucleic Acids, 47
- 2.3.1 DNA and RNA Building Blocks, 47
- 2.3.2 DNA and RNA Molecular Structures, 47
- 2.3.3 Transmission of Genetic Information, 53
- 2.3.4 Genetic Mutations and Site-Directed Mutagenesis, 56
- 2.3.5 Genes and Cloning, 58
- 2.3.6 Genomics and the Human Genome, 61

2.4 Zinc-Finger Proteins, 63
- 2.4.1 Descriptive Examples, 67

2.5 Summary and Conclusions, 73
References, 74

3 Instrumental Methods **76**

3.1 Introduction, 76
- 3.1.1 Analytical Instrument-Based Methods, 76
- 3.1.2 Spectroscopy, 77

3.2 X-Ray Absorption Spectroscopy (XAS) and Extended X-Ray Absorption Fine Structure (EXAFS), 78
- 3.2.1 Theoretical Aspects and Hardware, 78
- 3.2.2 Descriptive Examples, 81

3.3 X-Ray Crystallography, 83
- 3.3.1 Introduction, 83
- 3.3.2 Crystallization and Crystal Habits, 84
- 3.3.3 Theory and Hardware, 88
- 3.3.4 Descriptive Examples, 95

3.4 Nuclear Magnetic Resonance, 98
- 3.4.1 Theoretical Aspects, 98
- 3.4.2 Nuclear Screening and the Chemical Shift, 101
- 3.4.3 Spin–Spin Coupling, 104
- 3.4.4 Techniques of Spectral Integration and Spin–Spin Decoupling, 106
- 3.4.5 Nuclear Magnetic Relaxation, 107
- 3.4.6 The Nuclear Overhauser Effect (NOE), 108
- 3.4.7 Obtaining the NMR Spectrum, 110
- 3.4.8 Two-Dimensional (2D) NMR Spectroscopy, 111
- 3.4.9 Two-Dimensional Correlation Spectroscopy (COSY) and Total Correlation Spectroscopy (TOCSY), 112
- 3.4.10 Nuclear Overhauser Effect Spectroscopy (NOESY), 115
- 3.4.11 Multidimensional NMR, 116
- 3.4.12 Descriptive Examples, 117

3.5 Electron Paramagnetic Resonance, 122
- 3.5.1 Theory and Determination of g-Values, 122

- 3.5.2 Hyperfine and Superhyperfine Interactions, 127
- 3.5.3 Electron Nuclear Double Resonance (ENDOR) and Electron Spin-Echo Envelope Modulation (ESEEM), 129
- 3.5.4 Descriptive Examples, 129

3.6 Mössbauer Spectroscopy, 132
- 3.6.1 Theoretical Aspects, 132
- 3.6.2 Quadrupole Splitting and the Isomer Shift, 134
- 3.6.3 Magnetic Hyperfine Interactions, 136
- 3.6.4 Descriptive Examples, 137

3.7 Other Instrumental Methods, 139
- 3.7.1 Atomic Force Microscopy, 139
- 3.7.2 Fast and Time-Resolved Methods, 143
  - 3.7.2.1 Stopped-Flow Kinetic Methods, 143
  - 3.7.2.2 Flash Photolysis, 144
  - 3.7.2.3 Time-Resolved Crystallography, 146
- 3.7.3 Mass Spectrometry, 148

3.8 Summary and Conclusions, 153

References, 154

4 Computer Hardware, Software, and Computational Chemistry Methods 157

4.1 Introduction to Computer-Based Methods, 157

4.2 Computer Hardware, 157

4.3 Molecular Modeling and Molecular Mechanics, 160
- 4.3.1 Introduction to MM, 160
- 4.3.2 Molecular Modeling, Molecular Mechanics, and Molecular Dynamics, 161
- 4.3.3 Biomolecule Modeling, 166
- 4.3.4 A Molecular Modeling Descriptive Example, 167

4.4 Quantum Mechanics-Based Computational Methods, 170
- 4.4.1 Introduction, 170
- 4.4.2 Ab Initio Methods, 170
- 4.4.3 Density Function Theory, 171
- 4.4.4 Semiempirical Methods, 173

4.5 Computer Software for Chemistry, 174
- 4.5.1 Mathematical Software, 180

4.6 World Wide Web Online Resources, 181
- 4.6.1 Nomenclature and Visualization Resources, 181
- 4.6.2 Online Societies, Online Literature Searching, and Materials and Equipment Websites, 183

4.7 Summary and Conclusions, 185

References, 185

5 Group I and II Metals in Biological Systems: Homeostasis and Group I Biomolecules 189

- 5.1 Introduction, 189
- 5.2 Homeostasis of Metals (and Some Nonmetals), 192
  - 5.2.1 Phosphorus as Phosphate, 192
  - 5.2.2 Potassium, Sodium, and Chloride Ions, 193
  - 5.2.3 Calcium Homeostasis, 194
- 5.3 Movement of Molecules and Ions Across Membranes, 195
  - 5.3.1 Passive Diffusion, 195
  - 5.3.2 Facilitated Diffusion, 197
    - 5.3.2.1 Gated Channels, 197
  - 5.3.3 Active Transport—Ion Pumps, 197
- 5.4 Potassium-Dependent Molecules, 199
  - 5.4.1 Na^+/K^+ ATPase: The Sodium Pump, 199
  - 5.4.2 Potassium (K^+) Ion Channels, 203
    - 5.4.2.1 Introduction, 203
    - 5.4.2.2 X-Ray Crystallographic Studies, 205
- 5.5 Conclusions, 235
- References, 235

6 Group I and II Metals in Biological Systems: Group II 238

- 6.1 Introduction, 238
- 6.2 Magnesium and Catalytic RNA, 238
  - 6.2.1 Introduction, 238
  - 6.2.2 Analyzing the Role of the Metal Ion, 241
  - 6.2.3 The Group I Intron Ribozyme, 244
  - 6.2.4 The Hammerhead Ribozyme 261
- 6.3 Calcium-Dependent Molecules, 301
  - 6.3.1 Introduction, 301
  - 6.3.2 Calmodulin, 302
    - 6.3.2.1 Introduction, 302
    - 6.3.2.2 Calmodulin Structure by X-Ray and NMR, 303
    - 6.3.2.3 Calmodulin Interactions with Drug Molecules, 308
    - 6.3.2.4 Calmodulin–Peptide Binding, 313
    - 6.3.2.5 Conclusions, 326
- 6.4 Phosphoryl Transfer: P-Type ATPases, 327
  - 6.4.1 Introduction, 327
  - 6.4.2 Calcium P-Type ATPases, 327
    - 6.4.2.1 Ca^{2+}-ATPase Protein SERCA1a and the Ca^{2+}-ATPase Cycle, 329
- 6.5 Conclusions, 337
- References, 338

7 Iron-Containing Proteins and Enzymes 343

- 7.1 Introduction: Iron-Containing Proteins with Porphyrin Ligand Systems, 343
- 7.2 Myoglobin and Hemoglobin, 343
  - 7.2.1 Myoglobin and Hemoglobin Basics, 345
  - 7.2.2 Structure of the Heme Prosthetic Group, 347
  - 7.2.3 Behavior of Dioxygen Bound to Metals, 348
  - 7.2.4 Structure of the Active Site in Myoglobin and Hemoglobin: Comparison to Model Compounds, 349
  - 7.2.5 Some Notes on Model Compounds, 352
  - 7.2.6 Iron-Containing Model Compounds, 353
  - 7.2.7 Binding of CO to Myoglobin, Hemoglobin, and Model Compounds, 356
  - 7.2.8 Conclusions, 359
- 7.3 Introduction to Cytochromes, 359
- 7.4 Cytochrome P450: A Monooxygenase, 361
  - 7.4.1 Introduction, 361
  - 7.4.2 Cytochrome P450: Structure and Function, 363
  - 7.4.3 Cytochrome P450: Mechanism of Activity, 365
  - 7.4.4 Analytical Methods: X-Ray Crystallography, 369
  - 7.4.5 Cytochrome P450 Model Compounds, 372
    - 7.4.5.1 Introduction, 372
    - 7.4.5.2 A Cytochrome P450 Model Compound: Structural, 372
    - 7.4.5.3 Cytochrome P450 Model Compounds: Functional, 374
  - 7.4.6 Cytochrome P450 Conclusions, 382
- 7.5 Cytochrome b(6)f: A Green Plant Cytochrome, 382
  - 7.5.1 Introduction, 382
  - 7.5.2 Cytochrome b(6)f Metal Cofactor Specifics, 386
- 7.6 Cytochrome bc_1: A Bacterial Cytochrome, 388
  - 7.6.1 Introduction, 388
  - 7.6.2 Cytochrome bc_1 Structure, 389
  - 7.6.3 Cytochrome bc_1 Metal Cofactor Specifics, 391
  - 7.6.4 The Cytochrome bc_1 Q Cycle, 395
  - 7.6.5 Cytochrome bc_1 Inhibitors, 397
  - 7.6.6 Cytochrome bc_1 Conclusions, 408
- 7.7 Cytochromes c, 408
  - 7.7.1 Introduction, 408
  - 7.7.2 Mitochondrial Cytochrome c (Yeast), 411
  - 7.7.3 Mitochondrial Cytochrome c (Horse), 416
  - 7.7.4 Cytochrome c Folding, Electron Transfer, and Cell Apoptosis, 422
    - 7.7.4.1 Cytochrome c Folding, 422

        7.7.4.2 Electron Transfer in Cytochrome c and Its Redox Partners, 424
        7.7.4.3 Apoptosis, 427
    7.7.5 Cytochrome c Conclusions, 429
7.8 Cytochrome c Oxidase, 429
    7.8.1 Introduction, 429
    7.8.2 Metal-Binding Sites in Cytochrome c Oxidase, 432
    7.8.3 Dioxygen Binding, Proton Translocation, and Electron Transport, 434
    7.8.4 Cytochrome c Oxidase Model Compounds and Associated Analytical Techniques, 440
    7.8.5 Cytochrome c Oxidase Conclusions, 453
7.9 Non-Heme Iron-Containing Proteins, 454
    7.9.1 Introduction, 454
    7.9.2 Proteins with Iron–Sulfur Clusters, 454
        7.9.2.1 The Enzyme Aconitase 455
    7.9.3 Iron–Oxo Proteins, 458
        7.9.3.1 Methane Monooxygenases 459
7.10 Conclusions, 465
References, 466

Index **477**

PREFACE

This second edition of *Bioinorganic Chemistry: A Short Course* adopts the same philosophy as the first—that is, chapters of introductory material followed by chapters featuring detailed discussions of specific bioinorganic chemistry topics. This approach foregoes any attempt to exhaustively survey the enormous range of bioinorganic topics that occupy the attention and research of theoreticians and experimentalists currently engaged in the field. In this second edition, introductory Chapters 1 and 2 cover inorganic chemistry essentials and biochemistry fundamentals for bioinorganic chemistry students whose background in these topics may be less than ideal. Chapter 3 (Instrumental Methods) concentrates on the physical and analytical methods used to describe the bioinorganic systems discussed in Chapters 5 through 7. Chapter 4 (Computer Hardware, Software, and Computational Chemistry Methods) describes some of the vast array of computer hardware, software, and drawing, visualization, computational, and modeling programs used by every researcher studying bioinorganic systems. Computational chemistry, for instance, allows researchers to predict molecular structures of known and theoretical compounds and to design and test new compounds on computers rather than at the laboratory bench. Chapter 5 (Group I and II Metals in Biological Systems: Homeostasis and Group I Biomolecules) discusses the vital roles of sodium and potassium ions in maintaining cellular integrity, and features the Nobel Prize-winning work of Roderick MacKinnon's research group on potassium ion channels. More structural work by the MacKinnon group confirming the selectivity of potassium ion channels for K^+ over Na^+ can be found in a recent *Science* magazine article (*Science* 2006, **314**, 1004–1007). Chapter 6 (Group I and II Metals in Biological Systems: Group II) describes the importance of magnesium ions in catalytic RNA (ribozymes). Readers interested in the "RNA World hypothesis", a theory connecting the origin of life with self-replicating ribozymes, will want to read the recent article by Michael Robertson and William Scott (*Science* 2007, **315**, 1549–1553). A background perspective on this article has been written by Gerald Joyce (*Science* 2007, **315**, 1507–1508). In addition, Chapter 6 discusses two calcium-containing biomolecules—calmodulin, a primary receptor for intracellular calcium ions and a switch in Ca^{2+}-dependent signaling pathways, and Ca^{2+}-ATPase, a major player in muscle contraction-relaxation cycles. Chapter 7 (Iron Containing Proteins and Enzymes) devotes much of its descriptive material to proteins and enzymes that contain their iron ions within a heme ligand system. This chapter extends the first edition's discussion of myoglobin and hemoglobin, then reports on some members of the ubiquitous cytochrome family—cytochrome P450, a monooxygenase, cytochrome b(6)f, a green plant constituent, bacteria-based cytochrome bc_1, members of the cytochrome c superfamily, and cytochrome c oxidase (CcO), the terminal electron transferring enzyme in the mitochondrial respiratory chain. An update reported recently by the Collman group (*Science* 2007, **315**, 1565–1568) connects the redox-active centers of cytochrome c oxidase—Fe_{a3}, Cu_B, and tyr244—to the rapid accumulation of four electrons. The four accumulated electrons are needed to reduce dioxygen, O_2, to two oxide, O^{2-}, ions while avoiding the production of partially reduced, tissue-damaging superoxide, $O_2^{-\bullet}$, or peroxide, O_2^{2-}, ions. A shorter section in Chapter 7 discusses non-heme iron-containing proteins and enzymes, many of which, like aconitase, feature iron-sulfur clusters. Lastly, Chapter 7 reports on the enzyme methane monooxygenase (MMO), utilized by methanotrophic bacteria to oxidize methane to methanol with incorporation of one O_2 oxygen atom.

Many exciting bioinorganic topics are not covered in either the first or the present editions of *Bioinorganic Chemistry: A Short Course*. The new field of nanobioinorganic chemistry has become a prominent research area, especially in the medical field. Readers who wish to research this area might start with the review article: "Metal Nanoshells" in the *Annals of Biomedical Engineering* 2006, **34**(1), 15–22. In this article, Jennifer L. West and coworkers describe a new class of nanoparticles that have tunable optical properties. Chad Mirkin and coworkers describe oligonucleotide-modified gold nanoparticles that are being developed as intracellular gene regulation agents (*Science*, 2006, **312**, 1027–1030; *J. Am. Chem. Soc.* 2006, **128**(29), 9286–9287; *J. Am. Chem. Soc.* 2006, **128**(27), 8899–8903). These agents may eventually find applications in controlling the expression of specific proteins in cells for medical diagnostic and therapeutic purposes. The International Council on Nanotechnology (ICON) maintains a website at http://icon.rice.edu/research.cfm that includes links to other databases of interest, such as NIOSH (National Institute for Occupational Safety and Health) and the nanomedicine portal. ICON is particularly interested in informing researchers and nanotechnology users on environmental and safety issues related to this new, rapidly expanding field.

Readers interested in the connection between bioinorganic chemistry and catalysis might begin by reading an article entitled: “Better than Platinum? Fuels Cells energized by enzymes.” written by Marcetta Darensbourg, Michael Hall, and Jesse Tye (*Proc. Natl. Acad. Sci. U.S.A.* 2005, **102**(47), 16911–16912.) This article briefly describes the interest of bioinorganic chemists in the hydrogenase enzymes that biologically and reversibly accomplish proton reduction and dihydrogen oxidation. Since their discovery, hydrogenase enzymes, containing sulfur-bridged di-iron or nickel-iron active sites, have been presented as possible substitutes for expensive noble-metal based catalysts in the $2H^+ + 2e^- \leftrightarrow H_2$ reaction. More recently, these researchers have published studies of synthetic di-iron(I) complexes as structural models of reduced Fe-Fe hydrogenase (*Inorg. Chem.* 2006, **45**(4), 1552–1559) and computational studies comparing computed gas-phase and experimental solution phase infrared spectra of Fe-Fe hydrogenase active site models (*J. Comput. Chem.* 2006, **27**(12), 1454–1462).

Readers with a more structural biology bent might be interested in the 2006 achievement of Jennifer A. Doudna’s group at the University of California, Berkeley in obtaining the first crystal structure of Dicer, an enzyme that initiates RNA interference (RNAi). This work, published in *Science* (2006, **311**, 195–198), helps confirm that two metal ions—in the X-ray crystallographic structure, Er^{3+} substitutes for the naturally occurring Mn^{2+} ions—participate in Dicer’s catalytic mechanism.

Intense research continues on the complex enzyme nitrogenase, described in the first edition’s Chapter 6. New X-ray crystallographic results for nitrogenase have led to the probable positioning of an atom, most plausibly nitrogen, as a central ligand in nitrogenase’s FeMo-cofactor (Rees, D. C., et al. *Science* 2002, **297**, 1696–1700). X-ray crystallographic data are deposited in the Protein Data Bank (PDB) at http://www.rcsb.org/pdb with the accession number 1M1N. (Note that the third character is the numeral one and not the letter “I”.) More recently, the Rees research group has structurally identified conformational changes in the nitrogenase complex during adenosine triphosphate (ATP) turnover (*Science* 2005, **309**, 1377–1380, PDB: 2AFH, 2AFI, 2AFK). Concurrent with structural studies, the Brian M. Hoffman group at Northwestern University has trapped N_2-derived intermediates bound to nitrogenase and synchronized the number of electrons arriving at the active site with possible nitrogenase H^+-, $H^\bullet$-, or H_2-containing intermediates. (Lukoyanov, D., Barney, B. M., Dean, D. R., Seefeldt, L. C., Hoffman, B. M. *Proc. Natl. Acad. Sci. U.S.A.* 2007, **104**(5), 1451–1455; Barney, B. M., Lukoyanov, D., Yang, T. C., Dean, D. R., Hoffman, B. M., Seefeldt, L. C. *Proc. Natl. Acad. Sci. U.S.A.* 2006, **103**(46), 17113–17118.) An excellent article with many references, available from the Royal Society at http://www.journals.royalsoc.ac.uk as a free download, reviews the structural basis of nitrogen fixation. (Rees, D. C., Tezcan, F. A., Haynes, C. A., Walton, M.Y., Andrade, S., Einsle, O., Howard, J.B. *Phil. Trans. R. Soc. A* 2005, **363**, 971–984.) In April 2007, a search of PubMed, www.pubmed.gov, using the keyword nitrogenase and limiting the search to the journal *Proceedings of the National Academy of Sciences U.S.A.*, and to the years 2005–2007, yielded thirteen pertinent articles, of which those published online more than one year ago are available as free downloads.

Researchers continue to extend their ability to study and analyze complex bioinorganic systems as new experimental and instrumental methods are developed and current ones are improved. For instance, protein structure determination in solution by nuclear magnetic resonance, NMR, received a boost in 2006 through a technique developed at Tokyo Metropolitan University. This technique, stereo-array isotope labeling, SAIL, will make it possible to routinely determine protein structures at least twice as large as those being determined using current NMR methods (Kainosho, M., Torizawa, T., Iwashita, Y., Terauchi, T., Ono, A. M., Guntert, P. *Nature* 2006, **440**, 52–57, PDB: 1X02). The solution structure of the Ca^{2+}-containing protein calmodulin described in the *Nature* article, as determined by the SAIL method, is compared to X-ray crystallographic structures in Section 6.3.2.2—see especially Figure 6.23.

In some cases, the increasing complexity of bioinorganic systems studied, and the increasing sophistication of the analytical methods used, has led to controversy over the interpretation of biomolecular structures and behaviors. In this text, variations in experimental results and their interpretations among different research groups are found in the discussions of potassium ion channels (Section 5.4.2), group I intron ribozymes (Section 6.2.3), and the hammerhead ribozyme (Section 6.2.4). This author has attempted to present material on all existent interpretations by different research groups working in good faith to solve thorny experimental problems. All researchers, including newcomers to these complicated subjects, should maintain an open mind, a continuing interest in and exploration of the problems, and a civil manner of discourse within the scientific literature.

Admission of errors can be part of this discourse, although, to my knowledge, these have not been called for in the research areas mentioned in the previous paragraph. Recently, however, retractions appeared in *Science* magazine concerning incorrect interpretations of X-ray crystallographic data gathered on the MsbA protein, an important member of a class of molecules that use energy from adenosine triphosphate, ATP, to transport molecules across cell membranes—the so-called ABC transporters. The erroneous structures arose not because of any fault in the data collection scheme or the protein crystals themselves, but because of a faulty data-analysis program used to massage the data into visualized molecular structures. The incorrectly visualized MsbA protein structures were featured in at least five journal articles now being retracted (Miller, G., News of the Week, *Science* 2006, **314**, 1856–1857; Chang, G., Roth, C. B., Reyes, C. L., Pornillos, O., Chen, Y-J., Chen, A. P. Letters, *Science* 2006, **314**. 1875; Miller C. Letters *Science* 2007, **315**, 459. No MsbA protein structures, faulty or otherwise, are discussed in this text. However, as will be said numerous times herein, the techniques of X-ray crystallography provide snapshots of biomolecules frozen into a solid crystalline lattice, not a normal biomolecular physical state of being, and certainly not representative of every possible molecular conformation in the biological milieu. If errors in data interpretation are also introduced, one sees how incorrect biomolecule structure visualizations find their way into the literature. Confirmation of X-ray crystallographic structural results through experimental biochemistry and by the use of multiple analytical techniques—nuclear magnetic resonance (NMR), electron paramagnetic resonance (EPR), and Mössbauer spectroscopies to name a few—should always be sought by bioinorganic researchers.

Lastly, and importantly, researchers, academicians, and their students want to maintain ethical behaviors in their scientific endeavors. Although science practitioners have historically been self-policing in this regard, and continue to be so, science writers and thinkers now call for more consideration of ethical topics, especially for students in graduate and post-graduate years as well as for early-career scientists. Readers who wish more information on ethical issues may consult a recent article entitled: "A Code of Ethics for the Life Sciences" by Nancy Jones, an American Association for the Advancement of Science/National Institutes of Health (NIH) Science Policy Fellow and a faculty member at Wake Forest University School of Medicine. The article has been published in *Science and Engineering Ethics*, by Springer Netherlands, January 30, 2007, online at http://www.springerlink.com.

This text is appropriate for use in one-semester bioinorganic chemistry courses offered to fourth year undergraduate chemistry, biochemistry and biology majors or first year graduate students concentrating in inorganic and biochemical subject areas. After presentation of some introductory material in inorganic, biochemistry, and a review of selected instrumental and computer-based topics, I suggest choosing one to three bioinorganic chemistry topics from Chapters 5 through 7 for thorough discussion. Following that, students should be encouraged to choose their own bioinorganic topics for research and study. Their endeavors could lead to classroom presentations, laboratory experimentation, and submission of written term papers. Certainly, the subject area provides great opportunities for introducing the use of primary literature sources and the application of computer- and internet-based searching, visualization, and modeling techniques.

A website to accompany the second edition of *Bioinorganic Chemistry: A Short Course* can be found at http://chemistry.washcoll.edu/roat/. The website contains the book's table of contents, a listing of online resources organized by chapter and subject area, additional figures organized by chapter section (best viewed while studying the section's material), updated bibliographic references, study questions for each chapter, and communication links for questions, comments, and corrections submitted by instructors and students.

ROSETTE M. ROAT-MALONE
Washington College

ACKNOWLEDGMENTS

Many groups of people contributed to the creation and realization of this book. Thanks to former bioinorganic chemistry students, whose enthusiasm for the subject material inspired the book's manner of presentation. Professional colleagues at Washington College and other universities worldwide helped in many ways—as critical readers, and as advisers on important subject areas to be included. The book would not exist without the expert assistance of Wiley editors—Anita Lekhwani, Rebekah Amos, Danielle Lacourciere, Nancy Heimbaugh, and Dean Gonzalez. Lastly, I express heartfelt gratitude to family and friends for their patience during the many months of gestation.

1

INORGANIC CHEMISTRY ESSENTIALS

1.1 INTRODUCTION

Bioinorganic chemistry involves the study of metal species in biological systems. As an introduction to the basic inorganic chemistry needed for understanding bioinorganic topics, this chapter will discuss the essential chemical elements, the occurrences and purposes of metal centers in biological species, the geometries of ligand fields surrounding these metal centers, and ionic states preferred by the metals. Important considerations include equilibria between metal centers and their ligands and a basic understanding of the kinetics of biological metal–ligand systems. The occurrence of organometallic complexes and clusters in metalloproteins will be discussed briefly, and an introduction to electron transfer in coordination complexes will be presented. Since the metal centers under consideration are found in a biochemical milieu, basic biochemical concepts, including a discussion of proteins and nucleic acids, are presented in Chapter 2.

1.2 ESSENTIAL CHEMICAL ELEMENTS

Chemical elements essential to life forms can be broken down into four major categories: (1) bulk elements (H/H^+, C, N, $O^{2-}/O_2^{-\bullet}/O_2^{2-}$, P, S/S^{2-}); (2) macrominerals and ions (Na/Na^+, K/K^+, Mg/Mg^{2+}, Ca/Ca^{2+}, Cl^-, PO_4^{3-}, SO_4^{2-}); (3) trace

---

Bioinorganic Chemistry: A Short Course, Second Edition, by Rosette M. Roat-Malone
Copyright © 2007 John Wiley & Sons, Inc.

elements ($Fe/Fe^{II}/Fe^{III}/Fe^{IV}$, Zn/Zn^{II}, $Cu/Cu^{I}/Cu^{II}Cu^{III}$); and (4) ultratrace elements, comprised of nonmetals (F/F^{-}, I/I^{-}, Se/Se^{2-}, Si/Si^{IV}, As, B) and metals ($Mn/Mn^{II}/Mn^{III}/Mn^{IV}$, $Mo/Mo^{IV}/Mo^{V}/Mo^{VI}$, $Co/Co^{II}/Co^{III}$, $Cr/Cr^{III}/Cr^{VI}$, $V/V^{III}/V^{IV}/V^{V}$, $Ni^{I}/Ni^{II}/Ni^{III}$, Cd/Cd^{2+}, $Sn/Sn^{II}/Sn^{IV}$, Pb/Pb^{2+}, Li/Li^{+}). In the preceding classification, only the common biologically active ion oxidation states are indicated. (See references 3 and 21d for more information.) If no charge is shown, the element predominately bonds covalently with its partners in biological compounds, although elements such as carbon (C), sulfur (S), phosphorus (P), arsenic (As), boron (B), selenium (Se) have positive formal oxidation states in ions containing oxygen atoms; that is, S = +6 in the SO_4^{2-} ion or P = +5 in the PO_4^{3-} ion. The identities of essential elements are based on historical work and that done by Klaus Schwarz in the 1970s.[1] Other essential elements may be present in various biological species. Essentiality has been defined by certain criteria: (1) A physiological deficiency appears when the element is removed from the diet; (2) the deficiency is relieved by the addition of that element to the diet; and (3) a specific biological function is associated with the element.[2] Table 1.1 indicates the approximate percentages by weight of selected essential elements for an adult human.

Every essential element follows a dose–response curve, shown in Figure 1.1, as adapted from reference 2. At lowest dosages the organism does not survive, whereas in deficiency regions the organism exists with less than optimal function. After the concentration plateau of the optimal dosage region, higher dosages cause toxic effects in the organism, eventually leading to lethality. Specific daily requirements of essential elements may range from microgram to gram quantities as shown for two representative elements in Figure 1.1.[2]

Considering the content of earth's contemporary waters and atmospheres, many questions arise as to the choice of essential elements at the time of life's origins 3.5 billion or more years ago. Certainly, sufficient quantities of the bulk elements were available in primordial oceans and at shorelines. However, the concentrations of essential trace metals in modern oceans may differ considerably from those found in prebiotic times. Iron's current approximate 10^{-4} mM

TABLE 1.1 Percentage Composition of Selected Elements in the Human Body

Element	Percentage (by weight)	Element	Percentage (by weight)
Oxygen	53.6	Silicon, magnesium	0.04
Carbon	16.0	Iron, fluorine	0.005
Hydrogen	13.4	Zinc	0.003
Nitrogen	2.4	Copper, bromine	$2. \times 10^{-4}$
Sodium, potassium, sulfur	0.10	Selenium, manganese, arsenic, nickel	$2. \times 10^{-5}$
Chlorine	0.09	Lead, cobalt	$9. \times 10^{-6}$

Source: Adapted from reference 2.

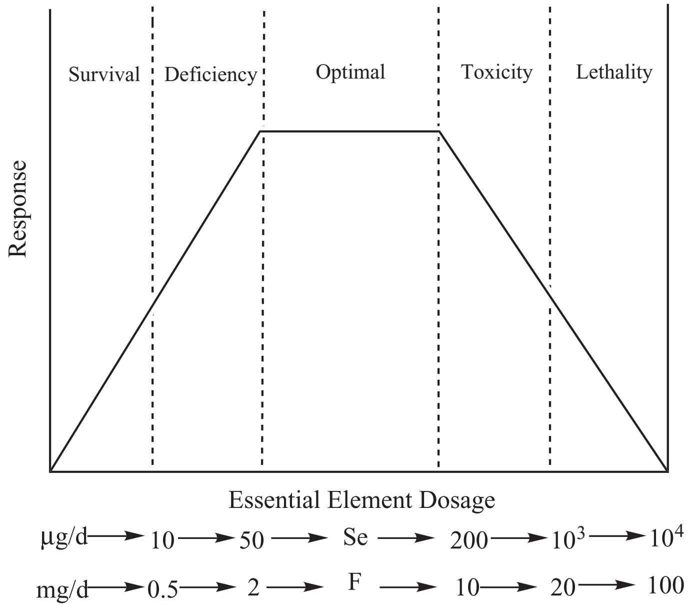

Figure 1.1 Dose–response curve for an essential element. (Used with permission from reference 2. Copyright 1985, Division of Chemical Education, Inc.)

concentration in seawater, for instance, may not reflect accurately its pre-life-forms availability. If one assumes a mostly reducing atmosphere contemporary with the beginnings of biological life, the availability of the more soluble iron(II) ion in primordial oceans must have been much higher. Thus, the essentiality of iron(II) at a concentration of 0.02 mM in the blood plasma heme (hemoglobin) and muscle tissue heme (myoglobin) may be explained. Besides the availability factor, many chemical and physical properties of elements and their ions are responsible for their inclusion in biological systems. These include: ionic charge, ionic radius, ligand preferences, preferred coordination geometries, spin pairings, systemic kinetic control, and the chemical reactivity of the ions in solution. These factors are discussed in detail by Frausto da Silva and Williams.[3]

1.3 METALS IN BIOLOGICAL SYSTEMS: A SURVEY

Metals in biological systems function in a number of different ways. Group 1 and 2 metals operate as structural elements or in the maintenance of charge and osmotic balance (Table 1.2). Transition metal ions that exist in single oxidation states, such as zinc(II), function as structural elements in superoxide dismutase and zinc fingers, or, as an example from main group +2 ions, as triggers for protein activity—that is, calcium ions in calmodulin or troponin C

TABLE 1.2 Metals in Biological Systems: Charge Carriers

Metal	Coordination Number, Geometry	Preferred Ligands	Functions and Examples
Sodium, Na^+	6, octahedral	*O*-Ether, hydroxyl, carboxylate	Charge carrier, osmotic balance, nerve impulses
Potassium, K^+	6–8, flexible	*O*-Ether, hydroxyl, carboxylate	Charge carrier, osmotic balance, nerve impulses

TABLE 1.3 Metals in Biological Systems: Structural, Triggers

Metal	Coordination Number, Geometry	Preferred Ligands	Functions and Examples
Magnesium, Mg^{2+}	6, octahedral	*O*-Carboxylate, phosphate	Structure in hydrolases, isomerases, phosphate transfer, trigger reactions
Calcium, Ca^{2+}	6–8, flexible	*O*-Carboxylate, carbonyl, phosphate	Structure, charge carrier, phosphate transfer, trigger reactions
Zinc, Zn^{2+} (d^{10})	4, tetrahedral	*O*-Carboxylate, carbonyl, *S*-thiolate *N*-imidazole	Structure in zinc fingers, gene regulation, anhydrases, dehydrogenases
Zinc, Zn^{2+} (d^{10})	5, square pyramid	*O*-Carboxylate, carbonyl, *N*-imidazole	Structure in hydrolases, peptidases
Manganese, Mn^{2+} (d^5)	6, octahedral	*O*-Carboxylate, phosphate, *N*-imidazole	Structure in oxidases, photosynthesis
Manganese, Mn^{3+} (d^4)	6, tetragonal	*O*-Carboxylate, phosphate, hydroxide	Structure in oxidases, photosynthesis

(Table 1.3). Transition metals that exist in multiple oxidation states serve as electron carriers—that is, iron ions in cytochromes or in the iron–sulfur clusters of the enzyme nitrogenase or copper ions in cytochrome c oxidase (Cu_A site), azurin and plastocyanin (Table 1.4); as facilitators of oxygen transport—that is, iron ions in hemoglobin or copper ions in hemocyanin (Table 1.5); and as sites at which enzyme catalysis occurs—that is, copper ions in superoxide dismutase or cytochrome c oxidase (Cu_B site), iron ions in heme a_3 of cytochrome c oxidase, or iron and molybdenum ions in nitrogenase (Table 1.6). Metal ions may serve multiple functions, depending on their oxidation state or location within the biological system so that the classifications in Tables 1.2–1.6 are necessarily incomplete, arbitrary, and/or overlapping.[4,5]

TABLE 1.4 Metals in Biological Systems: Electron Transfer

Metal	Coordination Number, Geometry	Preferred Ligands	Functions and Examples
Iron, Fe^{2+} (d^6)	4, tetrahedral	*S*-Thiolate	Electron transfer, nitrogen fixation in nitrogenases
Iron, Fe^{2+} (d^6)	6, octahedral	*O*-Carboxylate, alkoxide, oxide, phenolate	Electron transfer in oxidases
Iron, Fe^{3+} (d^5)	4, tetrahedral	*S*-Thiolate	Electron transfer, nitrogen fixation in nitrogenases
Iron, Fe^{3+} (d^5)	6, octahedral	*O*-Carboxylate, alkoxide, oxide, phenolate	Electron transfer in oxidases
Copper, Cu^+ (d^{10}), Cu^{2+} (d^9)	3, trigonal planar	*N*-Imidazole	Electron transfer in Type III heme–copper oxidases (Cu_B in cytochrome c oxidase, for example)
Copper, Cu^+ (d^{10}), Cu^{2+} (d^9)	4, tetrahedral	*S*-Thiolate, thioether, *N*-imidazole	Electron transfer in Type I blue copper proteins and Type III heme–copper oxidases (Cu_A in cytochrome c oxidase, for example)

TABLE 1.5 Metals in Biological Systems: Dioxygen Transport

Metal	Coordination Number, Geometry	Preferred Ligands	Functions and Examples
Copper, Cu^{2+} (d^9)	5, square pyramid 6, tetragonal	*O*-Carboxylate, *N*-imidazole	Type II copper oxidases, hydoxylases Type III copper hydroxylases, dioxygen transport in hemocyanin
Iron, Fe^{2+} (d^6)	6, octahedral	*N*-Imidazole, porphyrin	Dioxygen transport in hemoglobin and myoglobin

TABLE 1.6 Metals in Biological Systems: Enzyme Catalysis

Metal	Coordination Number, Geometry	Preferred Ligands	Functions and Examples
Copper, Cu^{2+} (d^9)	4, square planar	*O*-Carboxylate, *N*-imidazole	Type II copper in oxidases
Cobalt, Co^{2+} (d^7)	4, tetrahedral	*S*-Thiolate, thioether, *N*-imidazole	Alkyl group transfer, oxidases
Cobalt, Co^{3+} (d^6)	6, octahedral	*O*-Carboxylate, *N*-imidazole	Alkyl group transfer in vitamin B_{12} (cyanocobalamin)
Cobalt, Co^{2+} (d^7)	6, octahedral	*O*-Carboxylate *N*-imidazole	Alkyl group transfer in vitamin B_{12r}
Cobalt, Co^{+} (d^8)	6, octahedral, usually missing the 6th ligand	*O*-Carboxylate, *N*-imidazole	Alkyl group transfer in vitamin B_{12s}
Nickel, Ni^{2+} (d^8)	4, square planar	*S*-Thiolate, thioether, *N*-imidazole, polypyrrole	Hydrogenases, hydrolases
Nickel, Ni^{2+} (d^8)	6, octahedral		Uncommon
Molybdenum, Mo^{4+} (d^2), Mo^{5+} (d^1), Mo^{6+} (d^0)	6, octahedral	*O*-Oxide, carboxylate, phenolate, *S*-sulfide, thiolate	Nitrogen fixation in nitrogenases, oxo transfer in oxidases

1.4 INORGANIC CHEMISTRY BASICS

Ligand preference and possible coordination geometries of the metal center are important bioinorganic principles. Metal ligand preference is closely related to the hard–soft acid–base nature of metals and their preferred ligands. These are listed in Table 1.7.[6]

In general, hard metal cations form their most stable compounds with hard ligands, whereas soft metal cations form their most stable compounds with soft ligands. Hard cations can be thought of as small dense cores of positive charge, whereas hard ligands are usually the small highly electronegative elements or ligand atoms within a hard polyatomic ion—that is, oxygen ligands in $(RO)_2PO_2^-$, or $CH_3CO_2^-$. Crown ethers are hard ligands that have cavities suitable for encapsulating hard metal ions. The [18]-crown-6 ether shown in Figure 1.2 with its 2.6 to 3.2-Å hole provides a good fit for the potassium ion, which has a radius of 2.88 Å.[6]

It is possible to modify a hard nitrogen ligand toward an intermediate softness by increasing the polarizability of its substituents or the π electron cloud

TABLE 1.7 Hard–Soft Acid–Base Classification of Metal Ions and Ligands

Metals, Ions, Molecules				Ligands
HARD				HARD
H^+	Mg^{2+}	Al^{3+}	SO_3	Oxygen ligands in H_2O, CO_3^{2-}, NO_3^-, PO_4^{3-}, $ROPO_3^{2-}$, $(RO)_2PO_2^-$, CH_3COO^-, OH^-, RO^-, R_2O, and crown ethers Nitrogen ligands in NH_3, N_2H_4, RNH_2, or Cl^-
Na^+	Ca^{2+}	Co^{3+}	CO_2	
K^+	Mn^{2+}	Cr^{3+}		
	VO^{2+}	Ga^{3+}		
		Fe^{3+}		
		Tl^{3+}		
		Ln^{3+}		
		MoO^{3+}		
INTERMEDIATE				INTERMEDIATE
Fe^{2+}, Ni^{2+}, Zn^{2+}, Co^{2+}, Cu^{2+}, Pb^{2+}, Sn^{2+}, Ru^{2+}, Au^{3+}, SO_2, NO^+				Br^-, SO_3^{2-}, Nitrogen ligands in NO_2^-, N_3^-, N_2, 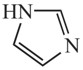 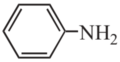
SOFT				SOFT
Cu^+	Pt^{2+}	Pt^{4+}		Sulfur ligands in RSH, RS^-, R_2S, R_3P, RNC, CN^-, CO, R^-, H^-, I^-, $S_2O_3^{2-}$, $(RS)_2PO_2^-$, $(RO)_2P(O)S^-$
Au^+	Pb^{2+}			
Tl^+	Hg^{2+}			
Ag^+	Cd^{2+}			
Hg_2^{2+}	Pd^{2+}			

Source: Adapted from references 4 and 6.

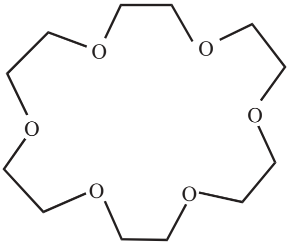

Figure 1.2 [18]-Crown-6 ether.

about it, an example being the imidazole nitrogen of the amino acid histidine. Increasing the softness of phosphate ion substituents can transform the hard oxygen ligand of $(RO)_2PO_2^-$ to a soft state in $(RS)_2PO_2^-$. Soft cations and anions are those with highly polarizable, large electron clouds—that is, Hg^{2+}, sulfur ligands as sulfides or thiolates, and iodide ions. Also, note that metal ions can overlap into different categories. Lead as Pb^{2+}, for instance, appears in both the intermediate and soft categories. The Fe^{3+} ion, classified as a hard cation, coordinates to histidine (imidazole) ligands in biological systems, whereas Fe^{2+}, classified as intermediate, can coordinate to sulfur ligands and the carbon atom of CO (see Section 7.2, for example, in which hemoglobin and myoglobin are discussed).

1.5 BIOLOGICAL METAL ION COMPLEXATION

1.5.1 Thermodynamics

The thermodynamic stability of metal ions is denoted by stepwise formation constants as shown in equations 1.1–1.3 (charges omitted for simplicity):

$$\mathrm{M} + \mathrm{L} \leftrightarrow \mathrm{ML} \qquad K_1 = \frac{[\mathrm{ML}]}{[\mathrm{M}][\mathrm{L}]} \tag{1.1}$$

$$\mathrm{ML} + \mathrm{L} \leftrightarrow \mathrm{ML_2} \qquad K_2 = \frac{[\mathrm{ML_2}]}{[\mathrm{M}][\mathrm{L}]} \tag{1.2}$$

$$\mathrm{ML_2} + \mathrm{L} \leftrightarrow \mathrm{ML_3} \qquad K_3 = \frac{[\mathrm{ML_3}]}{[\mathrm{ML_2}][\mathrm{L}]} \tag{1.3}$$

Alternately, they are indicated by overall stability constants as shown in equations 1.4–1.6:

$$\mathrm{M} + \mathrm{L} \leftrightarrow \mathrm{ML} \qquad \beta_1 = \frac{[\mathrm{ML}]}{[\mathrm{M}][\mathrm{L}]} \tag{1.4}$$

$$\mathrm{M} + 2\mathrm{L} \leftrightarrow \mathrm{ML_2} \qquad \beta_2 = \frac{[\mathrm{ML}]}{[\mathrm{M}][\mathrm{L}]^2} \tag{1.5}$$

$$\mathrm{M} + 3\mathrm{L} \leftrightarrow \mathrm{ML_3} \qquad \beta_3 = \frac{[\mathrm{ML}]}{[\mathrm{M}][\mathrm{L}]^3} \tag{1.6}$$

The equation relating the stepwise and overall stability constants is indicated by equation 1.7:

$$\beta_\mathrm{n} = K_1 K_2 \ldots \mathrm{K}_n \tag{1.7}$$

In biological systems, many factors affect metal–ligand complex formation. Hard–soft acid–base considerations have already been mentioned. Concentrations of the metal and ligand at the site of complexation are determined locally through concentration gradients, membrane permeability to metals and ligands, and other factors. Various competing equilibria—solubility products, complexation, and/or acid–base equilibrium constants—sometimes referred to as "metal ion speciation," all affect complex formation. Ion size and charge, preferred metal coordination geometry, and ligand chelation effects all affect metal uptake. To better measure biological metal–ligand interactions, an

TABLE 1.8 K_{ML} and $K_{ML} \times [M]$ for Some Cations and Their Differentiating Ligands

	K^+, Na^+	Ca^{2+}, Mg^{2+}	Zn^{2+}, Cu^{2+}	Differentiating Ligand
K^+, Na^+				*O*-Macrocycles such as crown ethers, cryptates and naturally occurring macrocyclic antibiotics such as nonactin and valinomycin
K_{ML}	>10	$<10^2$	$<10^6$	
$K_{ML} \times [M]$	>1.0	<0.1	<0.1	
Ca^{2+}, Mg^{2+}				Oxygen donors such as di- or tricarboxylates
K_{ML}	1.0	$<10^3$	$<10^6$	
$K_{ML} \times [M]$	<0.1	>1.0	<0.1	
Zn^{2+}, Cu^{2+}				Nitrogen and sulfur ligands
K_{ML}	0.1	$<10^2$	$>10^6$	
$K_{ML} \times [M]$	<0.1	<0.1	>1.0	

Source: Adapted from reference 3.

"uptake factor" is defined as $K_{ML} \times [M]$, where K_{ML} is the stability constant K_1 and [M] is the concentration of metal ion. Since naturally occurring aqueous systems have metal ion concentration varying roughly as

K^+, Na^+	Ca^{2+}, Mg^{2+}	Zn^{2+}	Cu^{2+}	Fe^{2+}
10^{-1} M	$\sim10^{-3}$ M	$<10^{-9}$ M	$<10^{-12}$ M	$\sim10^{-17}$ M

great selectivity for metal species is necessary to concentrate the necessary ions at sites where they are needed. Differentiating ligands are those preferred by the cation in question. A much more detailed discussion takes place in reference 3. Table 1.8 is adapted from this source.

1.5.2 Kinetics

As students learned in their introductory chemistry courses, rates of reaction are divided into several classes, depending on the number of reactants involved in rate determination. These are: (1) zero order—the reaction rate is independent of the concentration of that reactant; (2) first order—the reaction rate is dependent on the concentration of one reactant; (3) second order—the reaction rate is dependent on the concentration of two reactants; and (4) higher order—the reaction rate is dependent on more than two reactants. Higher-order reaction rates are very rare because the possibility of bringing more than two reactants together productively is very small. Bioinorganic kineticists, studying the reaction rates of complex enzymatic reactions, often simplify matters to isolate a reaction of interest and relate it to a proposed mechanism for the enzyme's catalytic activity. For instance, in a pseudo-zero-order reaction—that is, one that would be first order under normal circumstances—the concentration of the enzyme may be held constant while a particular substrate's concentration is varied but does not affect the reaction rate. This condition may apply when the enzyme is saturated with substrate over the range of substrate concentration studied. In a pseudo-first-order reaction—that is, one that would normally be second order—the concentration of one reactant is held constant while the other is varied so that the reaction rate is directly proportional to the reactant whose concentration is varied. This is the most commonly used experimental technique used by enzyme kineticists.

In biological systems, as in all others, metal ions exist in an inner coordination sphere, an ordered array of ligands binding directly to the metal. Surrounding this is the outer coordination sphere consisting of other ligands, counterions, and solvent molecules. In stoichiometric mechanisms where one can distinguish an intermediate, substitution within the metals inner coordination sphere may take place through an associative (A), S_N2 process as shown in equations 1.8 (for six-coordinate complexes) and 1.9 (for four-coordinate complexes) or a dissociative (D), S_N1 mechanism as shown in equation 1.10 (RDS = rate determining step).

$$ML_6^{n+} + L' \xrightarrow{\text{RDS}} ML_6L'^{n+} \rightarrow ML_5L'^{n+} + L \tag{1.8}$$

$$ML_4^{n+} + L' \xrightarrow{\text{RDS}} ML_4L'^{n+} \rightarrow ML_3L'^{n+} + L \tag{1.9}$$

$$ML_6^{n+} \xrightarrow{\text{RDS}} ML_5L^{n+} + L' \xrightarrow{\text{fast}} ML_5L'^{n+} + L \tag{1.10}$$

Associative mechanisms for metals in octahedral fields are difficult stereochemically (due to ligand crowding); therefore, they are rare for all but the largest metal ion centers. The associative mechanism is well known and preferred for four-coordinate square-planar complexes. Pure dissociative mechanisms are rare as well. When an intermediate cannot be detected by kinetic, stereochemical, or product distribution studies, the so-called interchange mechanisms (I) are invoked. Associative interchange (I_A) mechanisms have rates dependent on the nature of the entering group, whereas dissociative interchange (I_D) mechanisms do not.

The simplest reactions to study, those of coordination complexes with solvent, are used to classify metal ions as labile or inert. Factors affecting metal ion lability include size, charge, electron configuration, and coordination number. Solvents can by classified as to their size, polarity, and the nature of the donor atom. Using the water exchange reaction for the aqua ion $[M(H_2O)_n]^{m+}$, metal ions are divided by Cotton, Wilkinson, and Gaus[7] into four classes:

Class I. Rate constants for water exchange exceed $10^8 s^{-1}$, essentially diffusion controlled. These are classified as the labile species.

Class II. Rate constants for water exchange are in the range 10^4–$10^8 s^{-1}$.

Class III. Rate constants for water exchange are in the range 1–$10^4 s^{-1}$.

Class IV. Rate constants for water exchange are in the range 10^{-3}–$10^{-6} s^{-1}$. These ions are classified as inert.

Labile species are usually main group metal ions with the exception of Cr^{2+} (high-spin $3d^4$) and Cu^{2+} ($3d^9$) whose lability can be ascribed to Jahn–Teller

TABLE 1.9 Rate Constants for Water Exchange in Metal Aqua Ions

Class	Metal Ions	Rates log k (s^{-1})
I	Group IA (1), Group IIA (2) except Be and Mg, Group IIB (12) except Zn^{2+} ($3d^{10}$), Cr^{2+} ($3d^4$), Cu^{2+} ($3d^9$)	8–9
II	Zn^{2+} ($3d^{10}$)	7.6
	Mn^{2+} ($3d^5$)	6.8
	Fe^{2+} ($3d^6$)	6.3
	Co^{2+} ($3d^7$)	5.7
	Ni^{2+} ($3d^8$)	4.3
	Mg^{2+}	6.0
III	Ga^{3+}	3.0
	Be^{2+}	2.0
	V^{2+} ($3d^3$)	2.0
	Al^{3+}	<0.1
IV	Cr^{3+} ($3d^3$), Co^{3+} ($3d^6$), Rh^{3+} ($3d^6$), Ir^{3+} ($3d^6$), Pt^{2+} ($3d^8$)	−3 to −6

Source: Adapted from references 7 and 8.

effects. Section 1.6 includes a formula for determining the number of *d* electrons in a transition metal ion, and Figures 1.4 and 1.7 show the placement of *d* electrons into nondegenerate (split) *d* orbitals in various ligand fields. Jahn–Teller effects arise (for the high-spin $3d^4$ case) because the lone electron in the two destabilized, but degenerate, e_g orbitals causes further splitting of the e_g level with consequences for bond lengths between the metal ion and its ligands. Filling in the octahedral energy level diagram for the Cu^{2+} ($3d^9$) case in Figure 1.4, readers should be able to show three electrons in the e_g level, again causing a loss of degeneracy in these orbitals. Transition metals of classes II and III are species with small ligand field stabilization energies, whereas the inert species have high ligand field stabilization energies (LFSE). Examples include Cr^{3+} ($3d^3$) and Co^{3+} ($3d^6$). Jahn–Teller effects and LFSE are further discussed in Section 1.6. Table 1.9 reports rate constant values for some aqueous solvent exchange reactions.[8]

Outer-sphere (OS) reaction rates and rate laws can be defined for solvolysis of a given complex. Complex formation is defined as the reverse reaction—that is, replacement of solvent (S) by another ligand (L′). Following the arguments of Tobe,[9] in aqueous solution the general rate law for complex formation (eliminating charge for simplicity),

$$[M(L_n)(S)] + L' \rightarrow [M(L_n)(L')] + S \tag{1.11}$$

takes the second-order form shown in equation 1.12:

$$-d\frac{[M(L_n)(S)]}{dt} = k'[M(L_n)(S)][L'] \tag{1.12}$$

The rate law frequently may be more complex and given as equation 1.13:

$$-d\frac{[\mathrm{M(L}_n\mathrm{)(S)]}}{dt}=\frac{k'\mathrm{K[M(L}_n\mathrm{)(S)][L']}}{(1+\mathrm{K[L']}}\tag{1.13}$$

Equation 1.13 reduces to the second-order rate law, shown in equation 1.12, when $K[\mathrm{L}'] <<< 1$ and to a first-order rate law, equation 1.14,

$$-d\frac{[\mathrm{M(L}_n\mathrm{)(S)]}}{dt}=k'[\mathrm{M(L}_n\mathrm{)(S)]}\tag{1.14}$$

when $K[\mathrm{L}'] >>> 1$.

Interchange mechanisms ($\mathrm{I_A}$ or $\mathrm{I_D}$) in a preformed outer sphere (OS) complex will generate the following observed rate laws (which cannot distinguish $\mathrm{I_A}$ from $\mathrm{I_D}$) with the equilibrium constant = K_{OS} (equation 1.15) and $k = k_\mathrm{i}$ (equation 1.16).

$$[\mathrm{M(L}_n\mathrm{)(S)]}+\mathrm{L}'\leftrightarrow[\mathrm{M(L}_n\mathrm{)(S)]}\ldots\mathrm{L}'\qquad K_{\mathrm{OS}}\tag{1.15}$$

$$[\mathrm{M(L}_n\mathrm{)(S)]}\ldots\mathrm{L}'\rightarrow[\mathrm{M(L}_n\mathrm{)(L')]}\ldots\mathrm{S}\qquad k_i\tag{1.16}$$

The dissociative (D or S_N1) mechanism, for which the intermediate is long-lived enough to be detected, will yield equations 1.18 and 1.19 where $k = k_1$ and $K = k_2/(k_{-1}[\mathrm{S}])$. For the reaction:

$$\begin{aligned}&[\mathrm{M(L}_n\mathrm{)]}+\mathrm{S}\xrightarrow{k_1}[\mathrm{M(L}_n\mathrm{)(S)]},\text{ and its reverse,}\\&[\mathrm{M(L}_n\mathrm{)(S)]}\xrightarrow{k_{-1}}[\mathrm{M(L}_n\mathrm{)]}+\mathrm{S}\end{aligned}\tag{1.17}$$

$$[\mathrm{M(L}_n\mathrm{)(S)]}\leftrightarrow[\mathrm{M(L}_n\mathrm{)]}+\mathrm{S}\qquad k_1k_{-1}\tag{1.18}$$

$$[\mathrm{M(L}_n\mathrm{)]}+\mathrm{L}'\rightarrow[\mathrm{M(L}_n\mathrm{)(L')]}\qquad k_2\tag{1.19}$$

The associative (A or S_N2) will give the simple second-order rate law shown in equations 1.21 and 1.22 if the higher coordination number intermediate concentration remains small, resulting in the rate dependence shown in equation 1.23. For the reaction

$$\begin{aligned}&[\mathrm{M(L}_n\mathrm{)(S)]}+\mathrm{L}'\xrightarrow{k_a}[\mathrm{M(L}_n\mathrm{)(S)(L')]},\text{ and its reverse,}\\&[\mathrm{M(L}_n\mathrm{)(S)(L')]}\xrightarrow{k_{-a}}[\mathrm{M(L}_n\mathrm{)(S)]}+\mathrm{L}'\end{aligned}\tag{1.20}$$

we have

$$[\mathrm{M(L}_n\mathrm{)(S)]}+\mathrm{L}'\leftrightarrow[\mathrm{M(L}_n\mathrm{)(S)(L')]}\qquad k_ak_{-a}\tag{1.21}$$

$$[\mathrm{M(L}_n\mathrm{)(S)(L')]}\rightarrow[\mathrm{M(L}_n\mathrm{)(L')]}+\mathrm{S}\qquad k_b\tag{1.22}$$

$$-d\frac{[\mathrm{M(L}_n\mathrm{)(S)]}}{dt}=\frac{k_ak_b}{k_{-a}+k_b}[\mathrm{M(L}_n\mathrm{)(S)][L']}\tag{1.23}$$

In all cases the key to assigning mechanism is the ability to detect and measure the equilibrium constant K. The equilibrium constant K_{OS} can be estimated through the Fuoss–Eigen equation[10] as shown in equation 1.24. Usually, K_{OS} is ignored in the case of L' = solvent.

$$K_{\mathrm{OS}} = \frac{4\pi N_{\mathrm{A}} a^3}{3000}\left(e^{-V/kT}\right) \tag{1.24}$$

where a is the distance of closest approach of the oppositely charged ions (~5 Å), N_{A} is Avogadro's number, and V is the electrostatic potential at that distance (equation 1.25).

$$V = \frac{Z_1 Z_2 e^2}{4\pi\varepsilon_0\varepsilon_R a} \tag{1.25}$$

where

a = distance of closest approach of oppositely charged ions (~5 Å)

N_A = Avogadro's number, $6.022 \times 10^{23}\,\mathrm{mol}^{-1}$

V = electrostatic potential (dependent on distance between oppositely charged ions)

k = rate constant for a reaction

K = equilibrium constant for a reaction

$Z_1 Z_2$ = absolute value of the charge on an ion

e = charge on the electron, 4.8030×10^{-10} esu or 1.6022×10^{-19} Coulombs (C)

$\varepsilon_0\varepsilon_R$: ε_0 = permittivity in a vacuum 8.854×10^{-12} (C^2/Jm), ε_R or ε_r = dielectric constant = relative permittivity = 1 (for vacuum by definition, 80.4 for H_2O at 20°C), $\varepsilon_0\varepsilon_R$ = actual permittivity

As the above discussion indicates, assigning mechanisms to simple anation reactions of transition metal complexes is not simple. The situation becomes even more difficult for a complex enzyme system containing a metal cofactor at an active site. Methods developed to study the kinetics of enzymatic reactions according to the Michaelis–Menten model will be discussed in Section 2.2.4. Since enzyme-catalyzed reactions are usually very fast, experimentalists have developed rapid kinetic techniques to study them. Techniques used by bioinorganic chemists to study reaction rates will be further detailed in Section 3.7.2.1 and 3.7.2.2.

1.6 ELECTRONIC AND GEOMETRIC STRUCTURES OF METALS IN BIOLOGICAL SYSTEMS

Tables 1.2–1.6 list some of the important geometries assumed by metal ions in biological systems. Common geometries adopted by transition metal ions that will be of most concern to readers of this text are illustrated in Figure 1.3. It is important to remember that in biological systems these geometries are usually distorted in both bond length and bond angle.

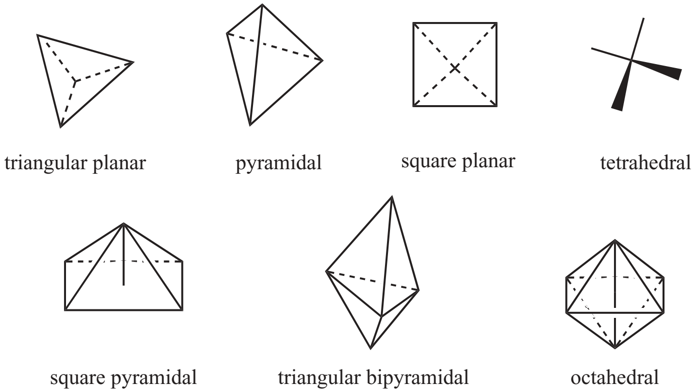
triangular planar

pyramidal

square planar

tetrahedral

square pyramidal

triangular bipyramidal

octahedral

Figure 1.3 Common transition metal coordination geometries.

Transition metal ions play special roles in biological systems, with all elements from the first transition series except titanium (Ti) and scandium (Sc) occurring with great variety in thousands of diverse metalloproteins. Metal ions determine the geometry of enzymatic active sites, act as centers for enzyme reactivity, and act as biological oxidation–reduction facilitators. Molybdenum (Mo) appears to be the only transition element in the second transition series with a similar role. Vanadium (V), technetium (Tc), platinum (Pt), ruthenium (Ru), and gold (Au) compounds, as well as gadolinium (Gd) and other lanthanide complexes, are extremely important in medicinal chemistry. Tables 1.2–1.6 list the *d* electron configuration for transition metal ions common to biological systems. To find the number of *d* electrons for any transition metal ion, the following is a useful formula:

Number of *d* electrons = Atomic number for the element (Z)
– oxidation state of the element's ion – Z for the preceding
noble-gas element.

Examples: Fe(II): 26 – 2 – 18 (argon) = 6
Mo(V): 42 – 5 – 36 (krypton) = 1

Note that there are a number of different methods for indicating the oxidation state of a metal ion, especially transition metal ions that have variable oxidation states. As an example, the iron ion in its +2 oxidation state may be written as Fe^{2+}, Fe(II), Fe^{II}, or iron(II). In this text, the methods are used interchangeably.

As a consequence of their partially filled *d* orbitals, transition metals exhibit variable oxidation states and a rich variety of coordination geometries and ligand spheres. Although a free metal ion would exhibit degenerate *d* electron energy levels, ligand field theory describes the observed splitting of these *d* electrons for metal ions in various ligand environments. In all cases, the amount of stabilization or destabilization of *d* electron energy levels centers about the

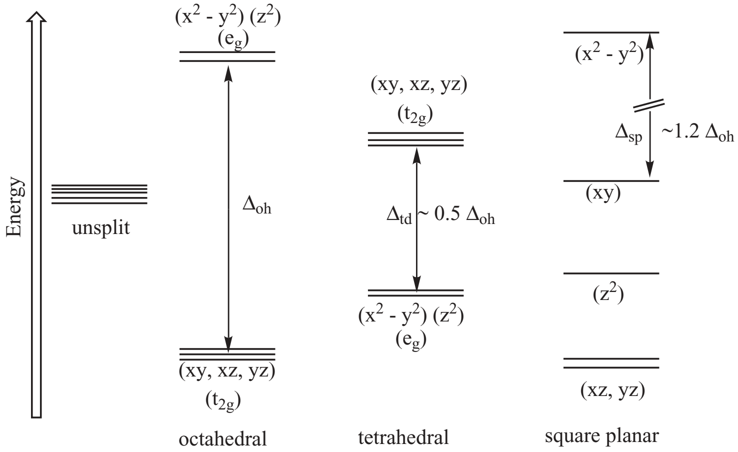

Figure 1.4 Approximate energy levels for *d* electrons in octahedral, tetrahedral, and square-planar fields.

so-called barycenter of unsplit *d* electron energy levels. The most important splittings for bioinorganic applications are shown in Figure 1.4 for octahedral, tetrahedral, and square-planar ligand fields. The t_{2g} (d_{xy}, d_{yz}, and d_{xz}) and e_g ($d_{x^2-y^2}$ and d_{z^2}) energy level designations identify symmetry properties of the *d* orbitals and are often used to indicate the degenerate energy levels under discussion. (See LFSE discussion below). Generally, the energy gap between stabilized and destabilized *d*-electron energy levels for tetrahedral fields (Δ_t) is approximately one-half that for octahedral fields (Δ_{oh}), and that for square-planar fields is approximately $1.2\Delta_{\mathrm{oh}}$. Many thermodynamic and kinetic properties of transition metal coordination complexes can be predicted by knowing the magnitude of Δ. Measurement of ultraviolet and visible absorption spectra of transition metal complexes that arise from these quantum mechanically forbidden (but observed) *d–d* transitions provide a measure of Δ.

To describe the *d*-orbital splitting effect for the octahedral field, one should imagine ligand spheres of electron density approaching along the *x*, *y*, and *z* axes where the $d_{x^2-y^2}$ and d_{z^2} lobes of electron density point. Figure 1.5 illustrates representations of high-probability electron orbit surfaces for the five *d* orbitals.

For octahedral (O_h) geometry the repelling effect of like charge approach of the ligand electrons toward regions of high *d* electron density along the *x, y*, and *z* axes elevates the energy of the e_g ($d_{x^2-y^2}$ and d_{z^2}) orbitals while the t_2g (d_{xy}, d_{yz}, and d_{xz}) orbitals are proportionally lowered in energy. For the tetrahedral (T_d) case ligands approach between the *x, y*, and *z* axes, stabilizing $d_{x^2-y^2}$ and d_{z^2} and destabilizing d_{xy}, d_{yz}, and d_{xz} orbital energy levels. For the square-planar case, ligands will approach along the *x* and *y* axes. Distorted octahedral and tetrahedral geometries are quite common in biological systems. Octahedral geometries are found for iron ions in heme ligand systems to be discussed in Chapter 7—for instance, while copper ions occur in distorted

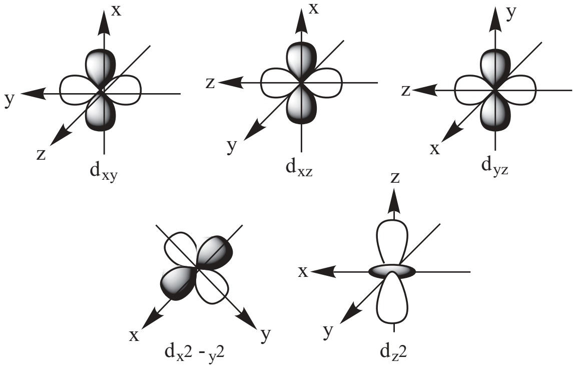

Figure 1.5 Representations of the five *d* orbitals along *x, y*, and *z* axes.

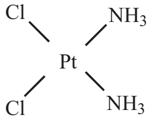

cis-dichlorodiammineplatinum(II)
cisplatin, cisDDP

Figure 1.6 The antitumor active platinum compound *cis*-dichlorodiammineplatinum (II).

pyramidal, tetrahedral, or even trigonal bipyramidal forms. Less commonly, square-planar geometries are found for d^8 transition metal ions, especially for gold(III), iridium(I), palladium(II), and platinum(II) and for nickel(II) species in strong ligand fields. The platinum anticancer agent, *cis*-dichlorodiammineplatinum(II), shown in Figure 1.6, has a square-planar geometry all important for its utilization as an antitumor agent. While the other geometries shown in Figure 1.3 might be less common for metal ions in biological species, they do occur (also with distorted bond distances and angles) and will be described in discussions of the metal center in the specific protein or enzyme.

The strength of the ligand field at a metal center is strongly dependent on the character of the ligand's electronic field and leads to the classification of ligands according to a "spectrochemical series" arranged below in order from weak field (halides, sulfides, hydroxides) to strong field (cyanide and carbon monoxide):

$$I^- < Br^- < S^{2-} < Cl^- < NO_3^- < OH^- \sim RCOO^- < H_2O \sim RS^- < NH_3 \sim \text{imidazole} < \text{en (ethylenediamine or diaminoethane)} < \text{bpy (2,2}'\text{-bipyridine)} < CN^- < CO$$

Ligand field strength may determine coordination geometry. For example, $NiCl_4^{2-}$ occurs as a tetrahedral complex (small splitting—small Δ_{td}), whereas

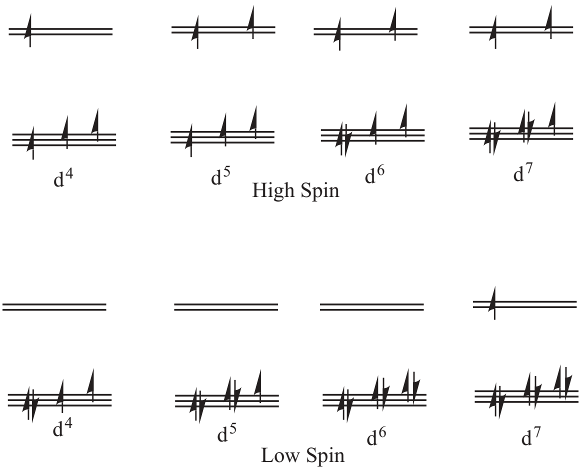

Figure 1.7 High-spin and low-spin *d*-electron configurations for the octahedral field.

$Ni(CN)_4^{2-}$ occurs in the square-planar geometry (large energy gap—large Δ_{sp}). In octahedral fields, ligand field strength can determine the magnetic properties of metal ions since for d^4 through d^7 electronic configurations both high-spin (maximum unpairing of electron spins) and low-spin (maximum pairing of electron spins) complexes are possible. Possible configurations are shown in Figure 1.7. In general, weak field ligands form high-spin (h.s.) complexes (small Δ_{oh}) and strong field ligands form low-spin (l.s.) complexes (large Δ_{oh}). Usually, tetrahedral complexes have high spin (small Δ_{td}) and will be paramagnetic. Square-planar complexes, usually found for metal ions having the electron configuration d^8, will be diamagnetic—all electrons paired—since a large energy gap occurs between the last filled orbital (d_{xy}) and the $d_{x^2-y^2}$ orbital (see Figure 1.4). Detection of paramagnetism (unpaired electrons) and diamagnetism (all electrons paired) in bioinorganic ligand fields can help determine coordination geometry at active enzymes sites. In the case of hemoglobin, for example, the d^6 iron(II) center cycles between high-spin (paramagnetic) and low-spin (diamagnetic) configurations. The change is evident in electron paramagnetic resonance (EPR) spectroscopy in which a spectrum is determined only for paramagnetic species. See Section 3.5. Placement of *d* electrons also affects the placement of the iron center in or out of the plane of its porphyrin ligand in hemoglobin or myoglobin—high-spin systems require more room so that a h.s. Fe(II) ion will move out of the porphyrin ligand's planar coordination sphere. See Section 7.2 for further discussion with respect to this phenomenon in myoglobin and hemoglobin. In Type III copper enzymes, two d^9 copper(II) centers become antiferromagnetically coupled resulting in a loss of the expected paramagnetism. See Section 7.8 for a discussion of binuclear copper centers in cytochrome c oxidase.

The sum of the *d* electron contributions to LFSE can be calculated with the formula shown in equation 1.26 for octahedral complexes.

$$\mathrm{LFSE} = \frac{2}{5}(\#\, e^{-} \text{ in } t_{2g})\Delta_{\mathrm{oh}} + \frac{3}{5}(\#\, e^{-} \text{ in } e_{g})\Delta_{\mathrm{oh}} \tag{1.26}$$

where $\#e^{-}$ is the number of *d* electrons.

The 2/5 stabilization (negative energy values) and 3/5 destabilization (positive energy values) modifiers arise from the displacement of three *d* orbitals to lower energy versus two *d* orbitals to higher energy from the unsplit degenerate *d* orbital state before imposition of the ligand field. Splitting values for *d* orbital energy levels, based on $\Delta_{\mathrm{oh}} = 10$, has been adapted from reference 7 and appears in Table 1.10.

The Jahn–Teller effect arises in cases where removal of degeneracy of a *d*-electron energy level is caused by partial occupation of a degenerate level. Two common examples are those of Cu(II), d^9, and high spin Cr(II), d^4, as shown in Figure 1.8. Electrons in the e_g level could be placed in either the $d_{x^2-y^2}$ and d_{z^2} orbitals. Placing the odd electron in either orbital destroys the degeneracy of the e_g orbitals and usually has the effect of moving the ligands on one axis in or out. For Cu(II) complexes this effect is very common, resulting in longer bond lengths on what is usually taken as the complex's *z* axis. The effect is also seen for high-spin d^4 Mn(III) and for low-spin d^7 Co(II) and Ni(III) complexes.

TABLE 1.10 Splitting Values for d Orbitals in Common Geometries

C. N.[a]	Geometry	$d_{x^2-y^2}$	d_{z^2}	d_{xy}	d_{xz}	d_{yz}
4	Tetrahedral	–2.67	–2.67	1.78	1.78	1.78
4	Square planar[b]	12.28	–4.28	2.28	–5.14	–5.14
5	Square pyramidal[c]	9.14	0.86	–0.86	–4.57	–4.57
6	Octahedral	6.00	6.00	–4.00	–4.00	–4.00

[a] C. N. stands for coordination number.
[b] Bonds in xy plane.
[c] Pyramidal base in *xy* plane.

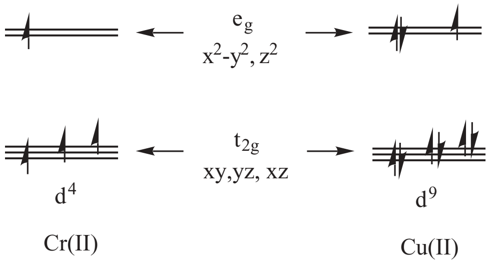

Figure 1.8 Electron configurations for high-spin Cr(II) and Cu(II).